IEEE Access
Multidisciplinary | Rapid Review | Open Access Journal

Date of publication xxxx 00, 0000, date of current version xxxx 00, 0000.

Digital Object Identifier xx..Doi Number xxs

Deep Learning of Sparse Patterns in Medical IoT for Efficient Big Data Harnessing

Junhua Wong, Qingxue Zhang, Senior Member, IEEE
Purdue University School of Engineering and Technology, Indiana, 46202, USA

Corresponding author: Qingxue Zhang (e-mail: qxzhang@purdue.edu).

ABSTRACT The long-term and continuous streaming of big data from medical Internet of Things (IoT), poses a great challenge for the battery-limited tiny devices. To address this challenge, we propose a novel framework for medical IoT data sparsification, leveraging both deep learning and optimal space searching. More specifically, the deep sparsification networks are designed to learn to extract key sparse patterns in the medical IoT data, by projecting the original data stream to a sparsified data representation. Further, the principles for designing deep encoding networks have been analyzed by an optimal space searching strategy, aiming to determine the best deep sparsification architecture that meets the energy constraint or sparsification error constraint. Compared with state-of-the-art approaches, our deep learning-based and space search-optimized framework shows a dramatic capability to tackle the power hungriness problem on medical IoT big data. This novel study, by enabling energy-efficient medical IoT big data sparsification, is expected to boost the continuous and long-term medical IoT applications, such as cardiac monitoring, thereby advancing precision medicine.

INDEX TERMS Big Data, Deep Learning, IoT Big Data, Space Search

I. INTRODUCTION

Medical Internet of Things (IoT) [1-10] are advancing various smart health applications [11-14]. The long-term and continuous streaming of big data from medical IoT is expected to broadly ignite emerging big data-driven precision medicine. We take a special interest in wearable Electrocardiogram (ECG)-based cardiac health monitoring [15-17], and will demonstrate a generalizable deep learning framework [18, 19] that can learn and extract the critical patterns in the data, for energy consumption minimization.

The medical IoT devices are expected to be play an increasingly important role in human or environmental health monitoring. Nevertheless, the challenges arises when these devices need to continuously transmit the data wirelessly to the smart phones, relays, or cloud. Frequent recharging the monitor is troublesome and impacts the long-term usage of the device. How to lower the energy need is a critical question for IoT monitoring applications.

Major components of an IoT device usually include the controller, the sensing module, the communication module, and the power management module. The former two can now be implemented with a very low energy consumption, nevertheless, the wireless module consumes significant, usually the majority of the energy. Therefore, one promising strategy is to lower the energy consumption of the wireless module with acceptable energy overhead. In this study, targeting (ECG) monitoring [20, 21], we will demonstrate how deep learning [22-25] enables efficient IoT big data streaming.

ECG is a vital sign of human health, and a critical biomarker of heart diseases, which is the leading cause of death in the world. There have been some previously reported studies on lowering the energy consumption of ECG monitors. Discrete Wavelet Transformation (DWT) has been a common practice in many studies [26-29], which firstly transforms the original signal to the time-frequency domain, and then selects out significant wavelet coefficients for transmission. The signal can then be reconstructed on the receiver side from the coefficient. Compressed Sensing (CS) [29-32] has also been applied and reported in various data compression studies. The conversion matrix is used to project the original signal to a sparse space. Discrete Cosine Transform (DCT) [33-35] is another widely used method for data compression. It uses the cosine waves to decompose the original signal.

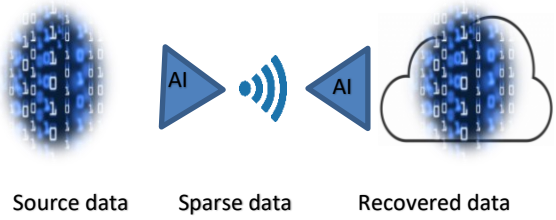

FIGURE 1. Deep learning of sparse patterns in medical IoT for efficient big data harnessing.

Interesting findings have been obtained in these previous studies. At the same time, current methods like DWT, DCT, and CS, are mainly using either predefined basis functions, or random conversion matrices, to perform the data projection. Nevertheless, the complex and nonlinear characteristics in the medical signals will benefit from more advanced and nonlinear methods in sparse pattern extraction. Another question that lack of comprehensive study is the overhead of the compression algorithm, which is crucial since the energy overhead may cancel out or even exceeds the energy saving on the big data transmission tasks.

In this study, we propose a novel and systematic AI-enabled framework, aiming to provide a data-driven, intelligent, and comprehensive methodology towards energy-efficient IoT applications as shown in Fig. 1. Our framework is leveraging both deep learning and optimal space searching. More specifically, the deep sparsification networks are designed to be able to learn the critical patterns in the IoT data, thereby projecting the original data stream to a sparsified data representation. Further, the principles for designing deep sparsification networks have been analyzed by an optimal space searching strategy, aiming to determine the best deep sparsification architecture with the energy constraint or sparsification error constraint.

Our major contributions include:

(a) Proposing a 'deep learning-based' and 'space search-optimized' framework for energy-efficient IoT big data streaming;

(b) Designing deep sparsification neural networks that can intelligently learn complex, critical dynamics in IoT data for effective pattern extraction;

(c) Developing optimal space search algorithms to determine optimal deep sparsification architectures under the energy constraint or sparsification error constraint;

(d) Validating the novel data-driven framework in the ECG-based cardiac health monitoring application, to demonstrate the feasibility and effectiveness.

This novel study, by enabling energy-efficient IoT big data streaming, is expected to boost the continuous and long-term IoT monitoring practices, thereby greatly advancing the big data-driven smart health and smart world.

II. APPROACHES

We here detail the proposed data-driven, intelligence systematic framework for energy-efficient IoT big data streaming. We will firstly give the system overview, then introduce the deep learning-based sparsification approach and the design variabilities, afterwards give the Optimal Deep Architecture Search (ODAS) algorithms with two typical kinds of constraints, and end this section with the system evaluation strategy.

A. SYSTEM OVERVIEW

The proposed novel system in given Fig. 2, where the top shows the deep learning-enabled dynamics sparsification approach, and the bottom illustrates the deep architecture search algorithms. More specifically, in Fig. 2(a), the IoT big data, i.e., ECG in this study, is projected to a sparsified representation, which is then wirelessly transmitted to the smart phone. The phone then recovers the original ECG

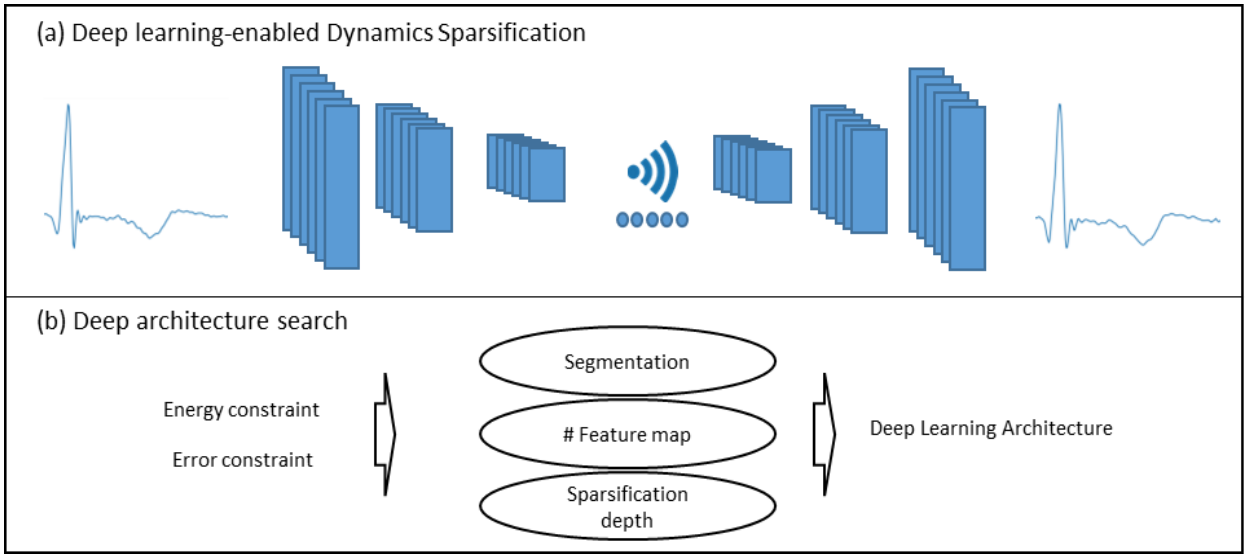

FIGURE. 2 The proposed novel framework for IoT big data streaming, leveraging (a) deep learning-enabled dynamics sparsification, and (b) deep architecture search of design variables with energy or error constraint.

signal from the sparse vector received, with an acceptable error. In such a way, the ECG data, after being sparsified, can consume much less energy compared with the case without sparsification or traditional approaches.

In Fig. 2(b), the ODAS algorithms search from the design variabilities the optimal deep sparsification architecture, with either energy constraint or error constraint. The resulted architectures will have minimum energy consumption or minimum error, respectively.

B. DEEP SPARSIFICATION

The proposed deep sparsification approach for ECG streaming is 1D Convolutional Autoencoder (CAE) [1-3]. CAE has two building blocks: the encoder and the decoder. The former one has multiple stages of convolutional filters to extract the key patterns in the ECG data X, as well as max pooling layers to reduce the dimensionality of the feature map. In such a way, the ECG signal is sparsified into a short vector S with critical patterns. The decoding process is given in (1), where X is the original signal with a length of N, and S is the sparse representation with a length of M. One thing to note is that we have designed the CAE to be 1D, meaning that the input image is 1D and the feature map is also 1D for temporal pattern extraction.

$$S = Encoder(X) \qquad (1)$$
$$X = \{x_i | i = 1, \dots N\}, S = \{s_j | j = 1, \dots M\}$$

Afterwards, on the smart phone, the sparse representation S is decoded as the estimate of the original signal, $\hat{X}$. The process is given in (2), where $\hat{X}$ also has a length of N.

$$\hat{X} = Decoder(S), \hat{X} = \{\hat{x_i} | i = 1, \dots N\} \qquad (2)$$

The promising advantage of the proposed 1D CAE is that it can effectively learn the patterns in the ECG data through deep neural learning and efficiently sparsify ECG with 1D operators. But CAE design has a high degree of design freedom, meaning that there are many variables which are related to sparsification error, energy reduction and energy overhead.

C. DEEP ARCHITECTURE VARIABILITIES

To further investigate how design factors of 1D CAE impact the sparsification error, energy reduction and energy overhead, we here select four critical design variabilities for the CAE architecture α, which is a function of input dimension I, feature map F, convolutional filter size C, and the depth D, as given in (3).

The sparsification ratio is determined by the depth D, i.e., the number of stages, since here we have fixed the maxpooling size of each stage to be two for convenient comparison. The sparsification error is related to all four variables. The total energy is related to the transmission energy reduction, the energy overhead of sparsification, and other system energy consumptions. Therefore, it is a nonlinear problem and thus the ODAS algorithms are proposed to solve this problem for determining the optimal architecture.

$$\alpha = \psi(I, F, C, D) \qquad (3)$$

D. OPTIMAL DEEP ARCHITECTURE SEARCH (ODAS)

The ODAS algorithms are proposed to solve the nonlinear problem of searching an optimal CAE architecture, given the complex design variables and their relationships to both error and total energy.

Two strategies are considered here: ODAS with energy constraint (ODAS-energy), and ODAS with sparsification error constraint (ODAS-error), given in (4) and (5), respectively. The former one, as shown in (4), searches an optimal CAE architecture α^{ε^*} with minimum error Z, while making sure the total energy ε is no more than a threshold ε_{th}.

$$\alpha^{\varepsilon^*} = \underset{\alpha}{argmin}\, Z(\alpha), s.t. \varepsilon \leq \varepsilon_{th} \qquad (4)$$

The second algorithm, i.e., ODAS-error as shown in (5), searches an optimal CAE architecture α^{ϵ^*} with minimum energy E, while making sure the sparsification error ϵ is no more than a threshold ϵ_{th}.

$$\alpha^{\epsilon^*} = \underset{\alpha}{argmin}\, E(\alpha), s.t. \epsilon \leq \epsilon_{th} \qquad (5)$$

We will then detail two ODAS algorithms, which can be used for different application scenarios, i.e., energy-constrained or error-constrained applications.

D. ODAS WITH SPARSIFICATION ENERGY CONSTRAINT

ODAS-energy handles the scenario which has an energy constraint, meaning that the total energy should not exceed a threshold.

ODAS-energy is detailed in Algorithm 1, which reads in the architecture variables and constraint, searches through the solution space, and returns the optimal CAE architecture. More specifically, the algorithm will first search through different CAE depths, since the depth directly determines the sparsification ratio and thus has major contributions to the energy reduction. However, when increasing the depth, the error usually increases. Therefore, the optimal architecture should correspond to appropriate depth that can meet the energy constraint while resulting in a small error. This will be further demonstrated in the results section, which will indicate that depth is the first degree of freedom where the ODAS-energy algorithm needs to explore.

Then, the ODAS-energy algorithm will search through the input dimension, i.e., the second degree of freedom, followed by the feature map and then the convolutional filter size. Considering the ECG database that we will use contains lots

Algorithm 1 ODAS-energy

Input:
input dimension $\Phi^I = \{I|I = 1, \dots, Imax\}$
feature map $\Phi^F = \{F|F = 1, \dots, Fmax\}$
convolutional filter size $\Phi^C = \{C|C = 1, \dots, Cmax\}$
depth $\Phi^D = \{D|D = 1, \dots, Dmax\}$
energy threshold ε_{th}

Output:
optimal architecture α^{ε^*}
error for the optimal architecture ϵ^{ε^*}
energy for the optimal architecture ε^*

Procedure:
$\alpha^{\varepsilon^*} = NULL$ //initialization
$\epsilon^{\varepsilon^*} = INFINITY$ //initialization
for $D = 1, \dots Dmax$ **do** //low to high
  for $I = 1, \dots, Imax$ **do** //low to high
    for $F = Fmax, \dots, 1$ **do** //high to low
      for $C = Cmax, \dots, 1$**do** //high to low
        $\varepsilon = \boldsymbol{E_{Tr}} + \boldsymbol{E_{Dl}} + \boldsymbol{E_{Sys}}$ //energy from wireless transmission, CAE overhead, and other system components
        if $\varepsilon \leq \varepsilon_{th}$ //energy threshold
          if $Z(\alpha) \leq \epsilon^{\varepsilon^*}$ //minimize error
            $\alpha^{\varepsilon^*} \leftarrow \psi(I, F, C, D)$
            $\epsilon^{\varepsilon^*} \leftarrow Z(\alpha)$
            $\varepsilon^* \leftarrow \varepsilon$
          end if
        end if
      end for
    end for
  end for
  if α^{ε^*} is not $NULL$ //stop searching depth
    break
  end if
end for
return $\alpha^{\varepsilon^*}, \epsilon^{\varepsilon^*}, \varepsilon^*$ //optimal architecture

of arrythmia heartbeats, the signal is highly diverse, which makes long-signal-segment sparsification challenging. So the algorithm searches the input dimension from low to high. Further, more feature maps and greater filter sizes usually yield lower reconstruction errors, we will search them from high to low.

By leveraging the proposed ODAS-energy algorithm we expect that the optimal CAE architecture can be effectively determined. The optimal architecture will not only meet the energy constraint but also own minimum sparsification error.

E. ODAS WITH ERROR CONSTRAINT

The ODAS-error algorithm aims to determine the optimal architecture that meets the sparsification error constraint while owns minimum energy. Here we mainly introduce the strategy of ODAS-error algorithm, which firstly search depth from high to low, i.e., the error is from high to low. Then the algorithm searches the input width, the feature map, and the convolutional filter size. More demonstrations will be given in the results section.

F. SYSTEM EVALUATION

To evaluate the proposed novel framework, we will study different CAE design parameters. The set of depth values Φ^D includes 2, 4 and 6 (sparsification ratio = 4/16/64, respectively); the set of input dimension values Φ^I includes 128, 256 and 512; the set of feature map values Φ^F includes 2, 4 and 6; the set of convolutional filter sizes Φ^C includes 2, 4, 8 and 12. Through this through evaluation, we aims to demonstrate the design principles of effective CAE and the ODAS algorithms proposed.

III. RESULTS

A. . EXPERIMENTAL SETUP

To evaluate the proposed framework, we here use the popular MIT-BIH Arrythmia ECG Database [4-6] and select ten subjects without severe motion artifacts. This database include not only arrhythmia but also other kinds of heart diseases, making the data sparsification very challenging. The sampling rate of ECG is 360Hz, and the signal is preprocessed by a band-pass filter (0.5 to 49.5 Hz) to remove the baseline wander and powerline interference. The ECG stream is segmented with a window size equal to the input width of CAE, depending on the simulation requirements. To minimize the engineering effort and maximize the generalization ability of the algorithm, the ECG heartbeat locations are not identified, meaning that the segmentation is random. We have conducted subject-wise evaluation, to investigate whether a subject's own data is sufficient for training the deep learning framework. In future, we will further consider other evaluation method like leave-one/more-subject out cross validation. 75% of each ECG stream is used for training and 25% for testing.

B. SPARSIFICATION RATIO VERSUS SPARSIFICATION ERROR

With different CAE depths, we can achieve various sparsification ratios, or compression ratios. Meanwhile, the corresponding sparsification errors also differ. Fig. 3 illustrates sparsification ratio versus sparsification Error, where CAE, DWT, ORI, CR and RMSE stand for convolutional autoencoder, discrete wavelet transform, original data without sparsification, compression ratio and root mean square error, respectively.

When increasing CR, for both CAE and DWT, RMSE increases since more non-critical patterns are filtered out for sparsification purpose. Under low CR, say 16, DWT show better performance, but when increasing CR to 32 or 64, CAE shows much better performance, thanks to CAE's

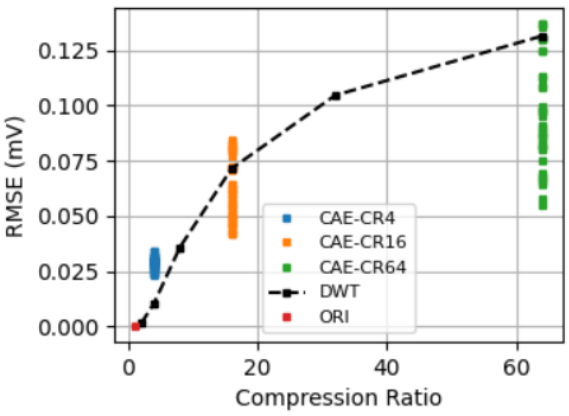

FIGURE. 3 Sparsification (compression) Ratio versus Sparsification Error.
Notes. CAE: convolutional autoencoder; DWT: discrete wavelet transform; ORI: original data without sparsification; CR: compression ratio; root mean square error.

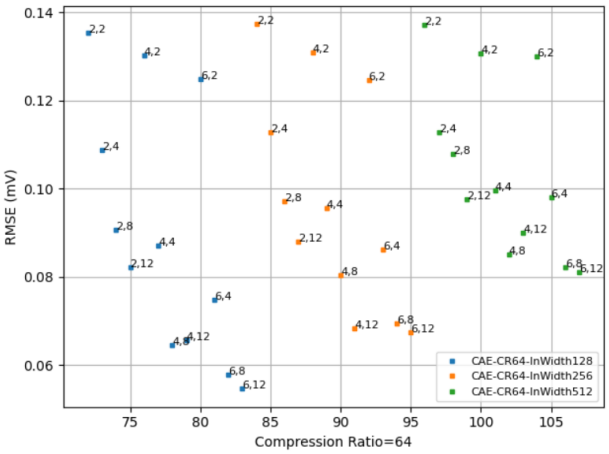

FIGURE. 4 Changes of Sparsification Error, under different input dimensions (128, 256, 512).
Notes. The top left dot 2, 2: #feature map, filter size; horizontal axis: scenario index; InWidth: input dimension.

intelligent removal of non-critical information in the ECG signal. This will be further illustrated later by the waveforms of the reconstructed signals.

Further, for CAE, there are multiple dots since there are combinations of different design variables. Take CR=64 as an example, the design variables, if chosen appropriately, can reduce RMSE dramatically.

Overall, the CAE approaches provide many solution candidates that have a less RMSE, given high compression ratios.

Next, we will analyze the contribution of different design variables to RMSE in detail.

C. DESIGN PRINCIPLE – INPUT DIMENSION

Fig. 4 shows the changes of sparsification error, under different input dimensions (128, 256, 512). The top left dot (2, 2) corresponds to (#feature map, filter size), and the horizontal axis gives the scenario indices. CR64 is selected to illustrate the details.

We can observe that the input dimension has a positive correlation with RMSE. It is because the disease ECG database is highly diverse, and if the input dimension is too high, it is much more challenging to reconstruct the diverse signals.

The complexity when considering the feature map and the convolutional figure size is further given below.

D. DESIGN PRINCIPLE – FEATURE MAP

Fig. 5 gives the changes of sparsification error, under different #feature map (2, 4, 6). The top left dot (128, 2) corresponds to (input dimension, filter size).

The #feature map, relatively speaking, has a negative correlation with RMSE, meaning that more feature maps can capture richer patterns from the original signal, thereby decreasing the error. Meanwhile, other design variables are also related to RMSE, resulting in a complex distribution of solution space.

E. DESIGN PRINCIPLE – CONVOLUTIONAL FILTER SIZE

Fig. 6 gives the sparsification error, under different filter sizes (2, 4, 8, 12). The top left dot (128, 2) corresponds to (input dimension, #feature map).

When increasing the convolutional filter size, RMSE basically decreases, indicating that a stronger ability to capture more spatial information contributes to signal reconstruction. Again, the complex distribution of solution space is related to all design variables. Besides, the design variables also generate different energy overhead.

F. TOTAL ENERGY VERS US SPARSIFICATION ERROR

Different CAE architectures make various contributions to the reconstruction error, however, for a specific sparsifcation ratio, we should not simply select the CAE architecture with the smallest error. This is because CAE also generated

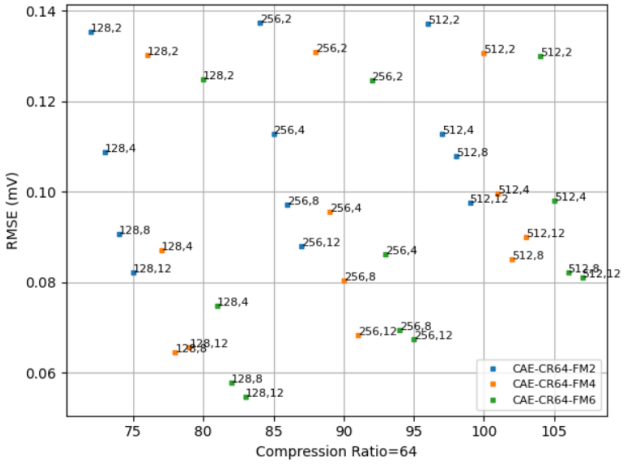

FIGURE. 5 Changes of Sparsification Error, under different #feature map (2, 4, 6).
Notes. The top left dot 128, 2: input dimension, filter size; horizontal axis: scenario index; FM: feature map.

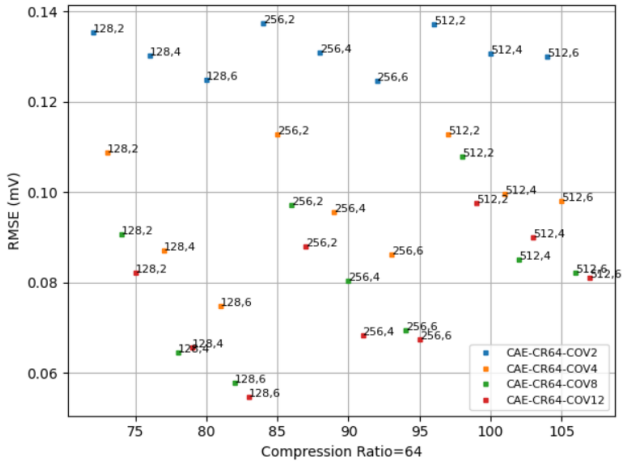

FIGURE. 6 Changes of Sparsification Error, under different filter sizes (2, 4, 8, 12).
Notes. The top left dot 128, 2: input dimension, #feature map; horizontal axis: scenario index; COV: convolutional filter size.

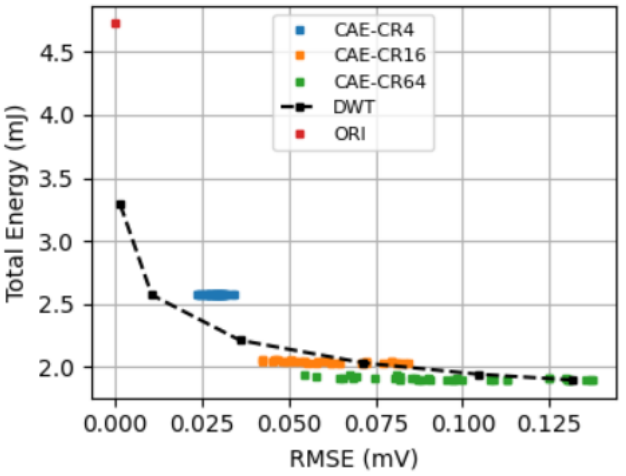

FIGURE. 7 Total Energy versus Sparsification Error.
Notes. CAE: convolutional autoencoder; DWT: discrete wavelet transform; ORI: original data without sparsification; CR: compression ratio.

energy consumption and we need to consider the overhead induced by CAE to the total energy.

In Fig. 7, total energy versus sparsification error is given. Encouragingly, for CAE-CR16 and CAE-CR-64, there are many CAE options that are better than the DWT options. These CAE solutions are under the DWT curve, indicating these solutions can offer lower RMSE with the same energy constraint, or offer lower energy with the same error constraint.

G. DESIGN PRINCIPLES WHEN CONSIDERING OVERHEAD

The zoomed in versions of these better CAE solutions are given in Fig. 8, 9 and 10, which illustrate the distribution of the solutions under different input dimensions, different #feature map, and different filter sizes, respectively. One thing to note is that these three figures show the same measurement distribution but with different annotation methods to highlight the contribution of different design parameters. In Fig. 8, we want to compare three input dimensions labeled with different colors, in Fig. 9, different #feature map is highlighted with different colors, and Fig. 10 highlights different filter sizes. These visualizations further show that the solution space is highly complex. But at the same time, some principles still hold: the smaller input dimensions, more feature maps, and larger filter sizes relatively give better solutions.

Therefore, we will later demonstrate that, by leveraging these principles, the proposed ODAS algorithm can effectively select the optimal CAE architectures.

To further demonstrate the performance of CAE and DTW, in Fig. 11, the recovered signals for different subjects and different approaches (CAE and DWT) are given. FM2/4/6 corresponds to CR4/16/64, respectively. We can observer that CAE significantly outperforms DWT.

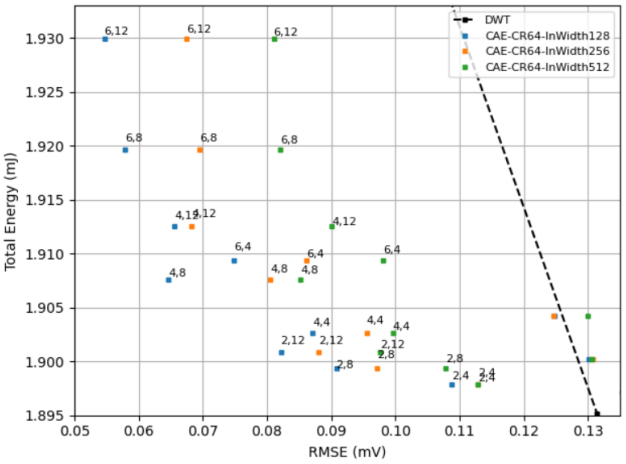

FIGURE. 8 Total Energy versus Sparsification Error, under different input dimensions (128, 256, 512).
Notes. The top left dot 6, 12: #feature map, filter size; horizontal axis: scenario index; InWidth: input dimension.

H. ODAS WITH SPARSIFICATION ENERGY

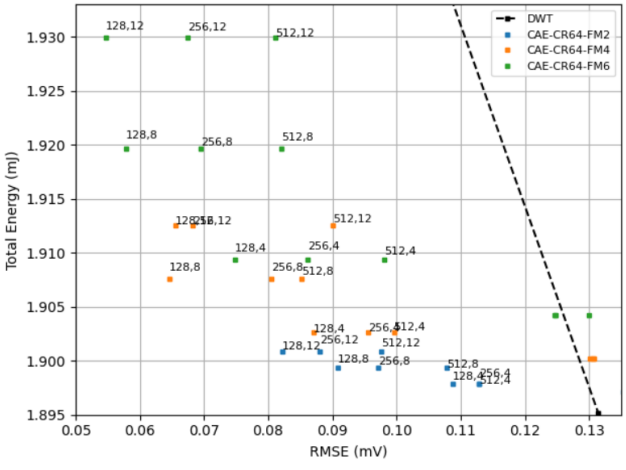

FIGURE. 9 Total Energy versus Sparsification Error, under different #feature map (2, 4, 6).
Notes. The top left dot 128, 2: input dimension, filter size; horizontal axis: scenario index; FM: feature map.

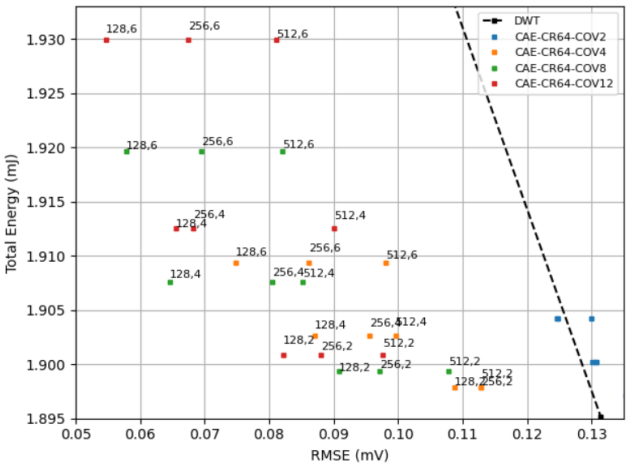

FIGURE. 10 Total Energy versus Sparsification Error, under different filter sizes (2, 4, 8, 12).
Notes. The top left dot 128, 2: input dimension, #feature map; horizontal axis: scenario index; COV: convolutional filter size.

CONSTRAINT

The ODAS-energy algorithm searches the solution space to determine the optimal CAE architecture that meets the energy constraint and owns the smallest sparsification error.

The comparison on the optimal CAE architecture with DWT is given in Fig. 12(a), which the energy constrain is set as 1.90 mJ. The sparsification error (RMSE) for DWT and CAE is 0.13 mV and 0.09 mV, respectively. The optimal CAE architecture is (128, 2, 8, 6), corresponds to (input dimension, #feature map, filter size, depth). So the sparsification ratio is 64. The optimal DWT architecture is CR64. This is in align with the solution space shown in Fig. 7, and detailed in Fig. 8, 9, and 10.

The algorithm first searches the CAE depth from low to high until the depth meets the requirements of the energy constraint. The algorithm then searches the in put dimension from low to high, the #feature map from high to low, and the filter size from high to low, respectively. Overall, ODAS-energy searches better solutions first based on the design principles, and if the current CAE depth provides at least one solution, it stops. For each depth, before search termination.

In such a way, the ODA-energy algorithm can determine an optimal solution that, not only meets the energy budget, but also has best combination of the design variables for error minimization.

I. ODAS WITH ERROR CONSTRAINT

The ODAS-error algorithm, similar to ODAS-energy, also searches the solution space to determine the CAE architecture. But different constraints usually yield different optimal solutions.

Fig. 12(b), where the error (RMSE) constraint is set as 0.08 mV, the optimal architecture for DWT and CAE has an energy consumption of 2.03 mJ and 1.91 mJ, respectively. The optimal CAE architecture is (128, 4, 8, 6), corresponds to (input dimension, #feature map, filter size, depth). So the sparsification ratio is 64. The optimal DWT architecture is CR16, indicating that DWT, to meet the error constraint,

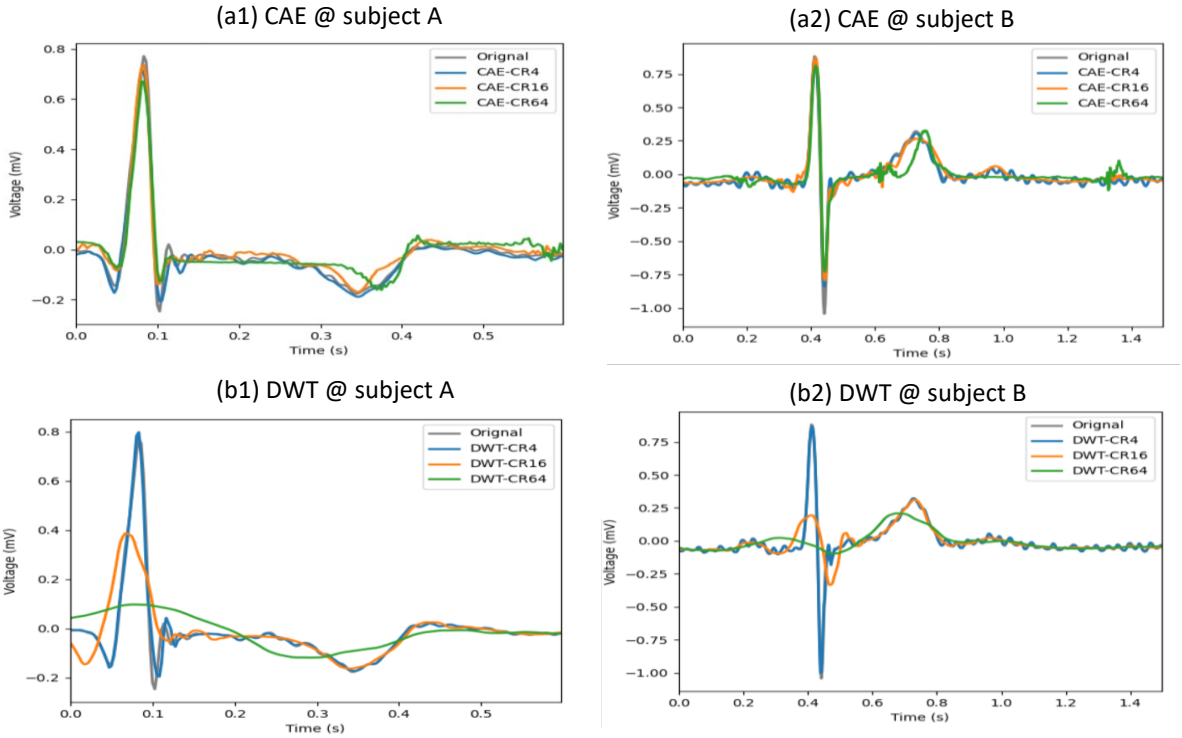

FIGURE. 11 The recovered signals for different subjects and different approaches (CAE and DWT), suggesting that CAE significantly outperforms DTW. FM2/4/6 corresponds to CR4/16/64, respectively.

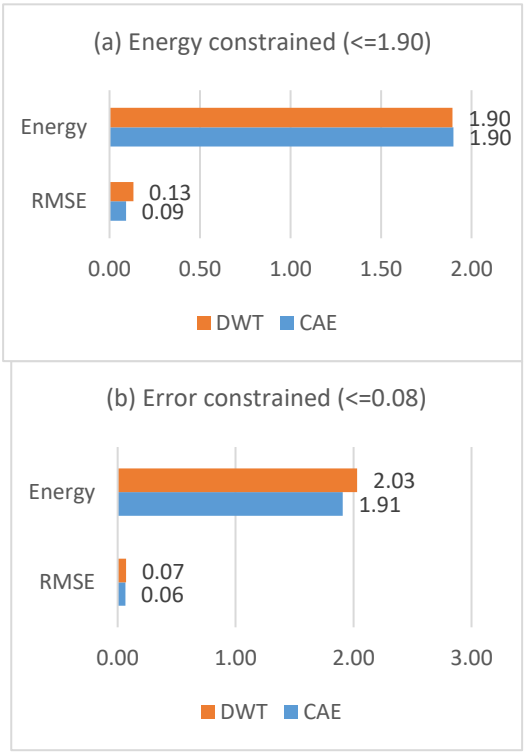

FIGURE. 12 The energy and error for the selected optimal architectures, under energy constraint (a) and error constriction, respectively.

can only decreases the sparsification ratio and increases the energy.

IV. CONCLUSION

IoT big data streaming is essential for data-driven smart health and smart world applications. Targeting the challenges induced by the power hungriness of IoT long-term streaming, we have proposed a deep learning-enabled big data sparsification framework. The novel framework can, not only sparsify the IoT data using intelligent autoencoder neural networks, but also determines the optimal deep learning architecture under the constraint. Compared with the traditional DWT data sparsification, the deep learning architecture determined by our framework provides better solutions, meaning that our framework can either offer the smallest error under the energy constraint, or offer the lowest energy under the error constraint. This research, validated on the ECG-based cardiac monitoring application, is expected to greatly advance IoT big data applications.

V. ACKNOWLEDGEMENT

This material is based upon work supported in part by the National Science Foundation (NSF) under the CAREER Award Grant 2047849. Any opinions, findings, and conclusions or recommendations expressed in this material are those of the author(s) and do not necessarily reflect the views of NSF.

REFERENCES

[1] Q. Zhang, L. T. Yang, Z. Chen, P. Li, and F. Bu, "An adaptive dropout deep computation model for industrial IoT big data learning with crowdsourcing to cloud computing," *IEEE Transactions on Industrial Informatics,* vol. 15, no. 4, pp. 2330-2337, 2018.

[2] P. Li, Z. Chen, L. T. Yang, Q. Zhang, and M. J. Deen, "Deep convolutional computation model for feature learning on big data in internet of things," *IEEE Transactions on Industrial Informatics,* vol. 14, no. 2, pp. 790-798, 2017.

[3] X. Xu and Q. Hua, "Industrial big data analysis in smart factory: Current status and research strategies," *Ieee Access,* vol. 5, pp. 17543-17551, 2017.

[4] S. Zeadally, F. Siddiqui, Z. Baig, and A. Ibrahim, "Smart healthcare: Challenges and potential solutions using internet of things (IoT) and big data analytics," *PSU research review,* 2019.

[5] M. Khan, X. Wu, X. Xu, and W. Dou, "Big data challenges and opportunities in the hype of Industry 4.0," in *2017 IEEE International Conference on Communications (ICC)*, 2017: IEEE, pp. 1-6.

[6] A. Yassine, S. Singh, M. S. Hossain, and G. Muhammad, "IoT big data analytics for smart homes with fog and cloud computing," *Future Generation Computer Systems,* vol. 91, pp. 563-573, 2019.

[7] M. Mohammadi, A. Al-Fuqaha, S. Sorour, and M. Guizani, "Deep learning for IoT big data and streaming analytics: A survey," *IEEE Communications Surveys & Tutorials,* vol. 20, no. 4, pp. 2923-2960, 2018.

[8] G. Manogaran, R. Varatharajan, D. Lopez, P. M. Kumar, R. Sundarasekar, and C. Thota, "A new architecture of Internet of Things and big data ecosystem for secured smart healthcare monitoring and alerting system," *Future Generation Computer Systems,* vol. 82, pp. 375-387, 2018.

[9] L. Farhan, S. T. Shukur, A. E. Alissa, M. Alrweg, U. Raza, and R. Kharel, "A survey on the challenges and opportunities of the Internet of Things (IoT)," in *2017 Eleventh International Conference on Sensing Technology (ICST)*, 2017: IEEE, pp. 1-5.

[10] M. Marjani *et al.*, "Big IoT data analytics: architecture, opportunities, and open research challenges," *ieee access,* vol. 5, pp. 5247-5261, 2017.

[11] M. Alkhodari, H. F. Jelinek, N. Werghi, L. J. Hadjileontiadis, and A. H. Khandoker, "Estimating Left Ventricle Ejection Fraction Levels Using Circadian Heart Rate Variability Features and Support Vector Regression Models," *IEEE Journal of Biomedical and Health Informatics,* vol. 25, no. 3, pp. 746-754, 2020.

[12] W. Zhang, L. Yu, L. Ye, W. Zhuang, and F. Ma, "ECG signal classification with deep learning for heart disease identification," in *2018 International Conference on Big Data and Artificial Intelligence (BDAI)*, 2018: IEEE, pp. 47-51.

[13] C. Venkatesan, P. Karthigaikumar, and S. Satheeskumaran, "Mobile cloud computing for ECG telemonitoring and real-time coronary heart disease risk detection," *Biomedical Signal Processing and Control,* vol. 44, pp. 138-145, 2018.

[14] S. C. Mukhopadhyay, S. K. S. Tyagi, N. K. Suryadevara, V. Piuri, F. Scotti, and S. Zeadally, "Artificial Intelligence-based Sensors for Next Generation IoT Applications: A Review," *IEEE Sensors Journal,* 2021.

[15] C. J. W. Borleffs *et al.*, "Predicting ventricular arrhythmias in patients with ischemic heart disease: clinical application of the ECG-derived QRS-T angle," *Circulation: Arrhythmia and Electrophysiology,* vol. 2, no. 5, pp. 548-554, 2009.

[16] D. Sapoznikov, M. H. Luria, Y. Mahler, and M. S. Gotsman, "Day vs night ECG and heart rate variability patterns in patients without obvious heart disease," *Journal of electrocardiology,* vol. 25, no. 3, pp. 175-184, 1992.

[17] D. De Bacquer, G. De Backer, M. Kornitzer, and H. Blackburn, "Prognostic value of ECG findings for total, cardiovascular disease, and coronary heart disease death in men and women," *Heart,* vol. 80, no. 6, pp. 570-577, 1998.

[18] Q. Zhang *et al.*, "IEEE Access Special Section Editorial: Smart Health Sensing and Computational Intelligence: From Big Data to Big Impacts," *IEEE Access,* vol. 9, pp. 30452-30455, 2021.

[19] Q. Zhang, V. Piuri, E. A. Clancy, D. Zhou, T. Penzel, and W. W. Hu, "IEEE Access Special Section Editorial: Advanced Information

Sensing and Learning Technologies for Data-Centric Smart Health Applications," *IEEE Access,* vol. 9, pp. 30404-30407, 2021.
[20] Q. Zhang and K. Frick, "All-ECG: a Least-Number of Leads ECG Monitor for Standard 12-Lead ECG Tracking During Motion," in *The 6th annual IEEE EMB Strategic Conference on Healthcare Innovations and Point-of-care Technologies (IEEE HI-POCT 2019)*, DC, USA, 2019 pp. 103-106.
[21] L.-H. Wang, T.-Y. Chen, K.-H. Lin, Q. Fang, and S.-Y. Lee, "Implementation of a wireless ECG acquisition SoC for IEEE 802.15. 4 (ZigBee) applications," *IEEE journal of biomedical and health informatics,* vol. 19, no. 1, pp. 247-255, 2014.
[22] J. Zou and Q. Zhang, "eyeSay: Make Eyes Speak for ALS Patients with Deep Transfer Learning-empowered Wearable," in *IEEE EMBS Annual Conference (Accepted)*, 2021: IEEE.
[23] J. Stauffer, Q. Zhang, and R. Boente, "DeepWave: Non-contact Acoustic Receiver Powered by Deep Learning to Detect Sleep Apnea," in *The 20th IEEE International Conference on BioInformatics And BioEngineering, USA* 2020.
[24] J. Stauffer, Q. Zhang, and A. Comer, "Deep Reconstruction Learning Towards Wearable Biomechanical Big Data," in *IEEE EMBS Conference on Biomedical Engineering and Sciences (IECBES 2021)*, 2020.
[25] J. Zou and Q. Zhang, "Intelligent Mobile Electrocardiogram Monitor-empowered Personalized Cardiac Big Data," in *The 11th IEEE Annual Ubiquitous Computing, Electronics and Mobile Communication Conference (IEEE UEMCON)*, 2020.
[26] Z. Lu, D. Y. Kim, and W. A. Pearlman, "Wavelet compression of ECG signals by the set partitioning in hierarchical trees algorithm," *IEEE transactions on Biomedical Engineering,* vol. 47, no. 7, pp. 849-856, 2000.
[27] J. Sahambi, S. Tandon, and R. Bhatt, "Using wavelet transforms for ECG characterization. An on-line digital signal processing system," *IEEE Engineering in Medicine and Biology Magazine,* vol. 16, no. 1, pp. 77-83, 1997.
[28] D. Mitra, H. Zanddizari, and S. Rajan, "Investigation of kronecker-based recovery of compressed ecg signal," *IEEE Transactions on Instrumentation and Measurement,* vol. 69, no. 6, pp. 3642-3653, 2019.
[29] V. Izadi, P. K. Shahri, and H. Ahani, "A compressed-sensing-based compressor for ECG," *Biomedical engineering letters,* vol. 10, no. 2, pp. 299-307, 2020.
[30] F. Pareschi *et al.*, "Energy analysis of decoders for rakeness-based compressed sensing of ECG signals," *IEEE transactions on biomedical circuits and systems,* vol. 11, no. 6, pp. 1278-1289, 2017.
[31] E. Balestrieri, L. De Vito, F. Picariello, and I. Tudosa, "A novel method for compressed sensing based sampling of ECG signals in medical-IoT era," in *2019 IEEE International Symposium on Medical Measurements and Applications (MeMeA)*, 2019: IEEE, pp. 1-6.
[32] J. Šaliga, I. Andráš, P. Dolinský, L. Michaeli, O. Kováč, and J. Kromka, "ECG compressed sensing method with high compression ratio and dynamic model reconstruction," *Measurement,* vol. 183, p. 109803, 2021.
[33] N. Soni, I. Saini, and B. Singh, "Morphologically Robust Discrete Cosine Transform based Lossless ECG Compression with Access Control Quality," in *2018 First International Conference on Secure Cyber Computing and Communication (ICSCCC)*, 2018: IEEE, pp. 289-293.
[34] A. Pandey, B. S. Saini, B. Singh, and N. Sood, "Quality controlled ECG data compression based on 2D discrete cosine coefficient filtering and iterative JPEG2000 encoding," *Measurement,* vol. 152, p. 107252, 2020.
[35] A. F. Hussein, A. K. AlZubaidi, A. Al-Bayaty, and Q. A. Habash, "An IoT real-time biometric authentication system based on ECG fiducial extracted features using discrete cosine transform," *arXiv preprint arXiv:1708.08189,* 2017.
[36] K. Mao, R. Tang, X. Wang, W. Zhang, and H. Wu, "Feature representation using deep autoencoder for lung nodule image classification," *Complexity,* vol. 2018, 2018.
[37] Y. Dai and G. Wang, "Analyzing tongue images using a conceptual alignment deep autoencoder," *IEEE Access,* vol. 6, pp. 5962-5972, 2018.
[38] W. Jia, M. Yang, and S.-H. Wang, "Three-category classification of magnetic resonance hearing loss images based on deep autoencoder," *Journal of medical systems,* vol. 41, no. 10, pp. 1-11, 2017.
[39] G. B. Moody and R. G. Mark, "The impact of the MIT-BIH arrhythmia database," *IEEE Engineering in Medicine and Biology Magazine,* vol. 20, no. 3, pp. 45-50, 2001.
[40] G. B. Moody and R. G. Mark, "A new method for detecting atrial fibrillation using RR intervals," *Computers in Cardiology,* vol. 10, no. 1, pp. 227-230, 1983.
[41] A. L. Goldberger *et al.*, "Physiobank, physiotoolkit, and physionet components of a new research resource for complex physiologic signals," *Circulation,* vol. 101, no. 23, pp. e215-e220, 2000.

JUNHUA WONG is a graduate student with Department of Electrical and Computer Engineering, Purdue University School of Engineering & Technology, USA. His research area includes smart health, deep learning, machine learning, signal processing, internet of things, big data, and efficient computing technologies.

QINGXUE ZHANG (Senior Member, IEEE) has over fifteen years' experience in both academia and industry, with his postdoc research at Harvard, products R&D in ICT, and Ph.D. research at University of Texas at Dallas. He is a faculty with Purdue University School of Engineering & Technology, USA. He is directing the Ubiquitous Intelligence Lab, with research interests including Deep Learning, IoT/Wearable, Edge Computing, and Brain-inspired Learning, targeting smart health, home, and world applications.

He is a recipient of the prestigious USA NSF CAREER Award. He serves as USA NSF/NIH/NIST Panelists, AE for IEEE Access, and committee for multiple IEEE conferences. He received the Featured Journal Article Award in IEEE Access, the Best Paper Award in UEMCON2017, the Early-Career Travel Award in AHA2020, the Favorite Professor Award in 2019, and the Google Cloud Award in 2019. He is a senior member of IEEE.